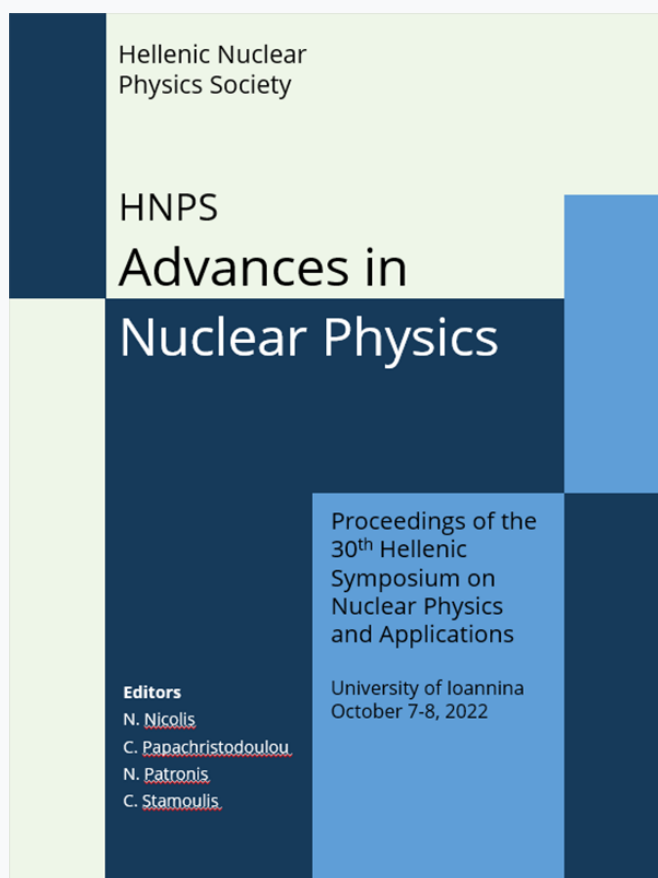


HNPS Advances in Nuclear Physics

Vol 29 (2023)

HNPS2022



Semiconductor Detector Study for Detecting Fusion Neutrons using Geant4 Simulations

Kalliopi Kaperoni, Maria Diakaki, Michael Kokkoris, Michael Axiotis, Anastasia Ziagkova, Christina Weiss, Roza Vlastou

doi: [10.12681/hnpsanp.5184](https://doi.org/10.12681/hnpsanp.5184)

Copyright © 2023, Kalliopi Kaperoni, Maria Diakaki, Michael Kokkoris, Michael Axiotis, Anastasia Ziagkova, Christina Weiss, Roza Vlastou



This work is licensed under a [Creative Commons Attribution-NonCommercial-NoDerivatives 4.0](https://creativecommons.org/licenses/by-nc-nd/4.0/).

To cite this article:

Kaperoni, K., Diakaki, M., Kokkoris, M., Axiotis, M., Ziagkova, A., Weiss, C., & Vlastou, R. (2023). Semiconductor Detector Study for Detecting Fusion Neutrons using Geant4 Simulations. *HNPS Advances in Nuclear Physics*, 29, 58–65. <https://doi.org/10.12681/hnpsanp.5184>

Semiconductor Detector Study for Detecting Fusion Neutrons using Geant4 Simulations

K. Kaperoni^{1*}, M. Diakaki¹, M. Kokkoris¹, M. Axiotis², A. Ziagkova¹, C. Weiss^{3,4}, R. Vlastou¹

¹ Department of Physics, National Technical University of Athens

² Tandem Accelerator Laboratory, Institute of Nuclear and Particle Physics

³ TU Wien, Atominstitut

⁴ CIVIDEC Instrumentation GmbH, 1010 Wien, Austria

Abstract Accurate neutron flux measurements in fusion reactors are essential, in order to determine the feasibility and progress of the reaction, as well as for safety issues. Semiconductor neutron detectors exhibit promising characteristics for operation in the extreme environmental conditions of fusion reactors. Silicon, Diamond and Silicon Carbide are the most studied and anticipated materials for constructing detectors with high efficiency and irradiation resistance. The ITER fusion reactor is expected to run D-D plasma measurements in the near future, so the detection of 2.45 MeV neutrons with appropriate detectors is of great and immediate importance. In the present work, the study of 2.45 MeV neutrons interactions with a silicon, diamond and silicon carbide detector was made, using GEANT4 [1] simulations, in order to compare their response. An experimental study will follow at the neutron production facility of the TANDEM accelerator of the I.N.P.P. of the NCSR “Demokritos”, with detectors provided by CIVIDEC Instrumentation GmbH, so the geometry of the simulations was built accordingly. In the simulations a quasi-monoenergetic neutron beam of 2.45 MeV was produced through $^3\text{H}(p,n)$ reactions in a TiT target. Due to the low cross section of the reaction, biasing techniques were implemented in the simulation to increase the counting rate, thus producing realistic results. These biasing techniques were studied with various tests and the parameters affecting the choice of the biasing factor are shown and discussed.

Keywords GEANT4, biasing, ITER, neutrons, fusion

INTRODUCTION

Since 2005, ITER (International Thermonuclear Experimental Reactor), the first experimental fusion reactor, is being built in France, in order to produce energy through D-T fusion. For the upcoming years, tests will be performed with D-D plasma, which results to the production of 2.45 MeV neutrons, while in 2035, D-T fusion experiments are going to begin, producing 14 MeV neutrons, according to ITER schedule. The feasibility of fusion is determined by the neutrons produced during the reaction. In D-T fusion, the produced neutron acquires 80% and in D-D fusion, 75% of the total energy [2], therefore the neutrons are energy carriers and the only output during fusion. Consequently, constructing special neutron detectors, with increased efficiency and irradiation resistance is of great importance.

Over 40 diagnostic systems are proposed to be installed at ITER in various locations, as shown in Fig. 1. These diagnostic systems will have to withstand: high neutron flux (up to 10^{14} n/cm² with 14 MeV neutrons, for D-T fusion), high temperatures due to plasma irradiation, magnetic fields up to 6T as well as electromagnetic noise due to auxiliary radiofrequency heating systems. More analytically, during full power discharges of ITER, 10^{21} n/cm² fusion neutrons per second will be produced and the fluxes in the locations of the different sensors will reach up to 10^9 n/cm² – 10^{14} n/cm². A large number of detectors will be placed in the vacuum vessel and in the port plugs which will be constantly held at temperatures from 70°C to 100°C. During shutdown periods, the vacuum vessel will be baked for tritium removal at 200°C and the divertor at 340°C. Neutron detectors in these areas will typically need to survive vacuum vessel baking. No maintenance is foreseen for these detectors for the whole ITER life cycle, so there is a great need for resilient materials able to withstand these harsh environmental

* Corresponding author: k.kaperoni@gmail.com

conditions [3]. Development of such detectors is a technological challenge and the research is ongoing. In this work, semiconductor detectors based on diamond (C), Si and SiC were studied, in order to compare their response to 2.45 MeV neutrons deriving from D-D fusion.

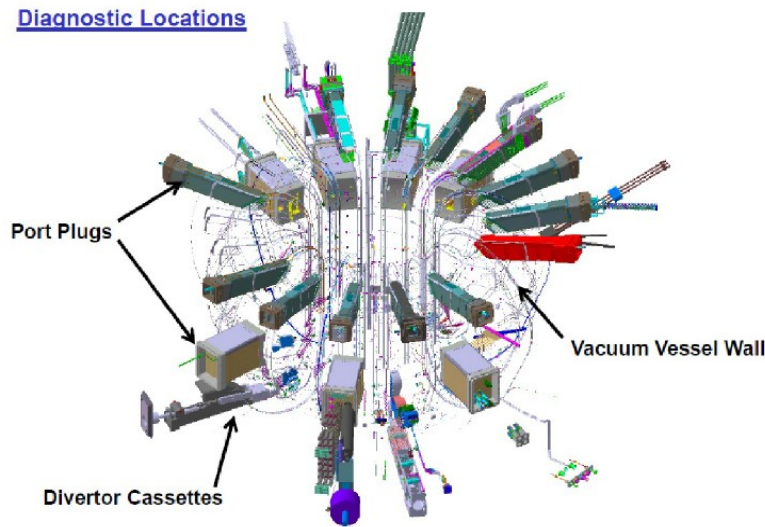


Figure 1. *Diagnostics locations at ITER [4]*

Silicon is a preferable material for neutron detection as it has a relatively low Z and thus low γ -ray interaction probability, low manufacturing cost and, above all, a high technological know-how thanks to the microelectronics industry based on silicon. Diamond exhibits excellent electrical and physical properties, the most noteworthy being its high bandgap energy and thermal conductivity, contributing to the high energy resolution and irradiation resistance. Lastly, SiC has material advantages such as elevated chemical and radiation tolerance, making it suitable to operate in extreme environmental conditions.

In the next sections, the study of neutron interactions with these three materials is described using the GEANT4 simulation toolkit [1]. The geometry was built according to the set-up of NCSR “Demokritos”, where the experiment will be conducted in the near future, using detectors and electronics provided by the CIVIDEC Instrumentation GmbH.

SIMULATION DETAILS

Monoenergetic Neutron Beam

For the simulation, a solid volume detector with dimensions $4\text{ mm} \times 4\text{ mm} \times 50\text{ }\mu\text{m}$ was built along with the description of the materials for each sensor. The physics list used was the QGSP-BIC which focuses on hadronic elastic, inelastic and capture processes. A monoenergetic neutron pencil beam of 10^9 primary particles, with energy of 2.45 MeV, was used to examine the energy deposition spectrum of the C, Si and SiC detectors.

Figure 2 represents the energy deposition spectrum for C, Si and SiC. According to kinematics, all spectra are dominated by neutron elastic scattering on C or Si nuclei. In Si and SiC there are additional α particles and Mg nuclei, deriving from $^{29}\text{Si}(n,\alpha)^{26}\text{Mg}$ reactions, occurring with very low probability. We observe the characteristic cut-off at the maximum deposited energy for the elastic scattering at 0.7 MeV for C and at 0.3 MeV for Si, whereas SiC combines the behavior of both nuclei. The counts above these energies are caused by neutron double scattering effects inside the detector, due to its non-negligible dimensions, causing each spectrum to extend in higher energies than expected.

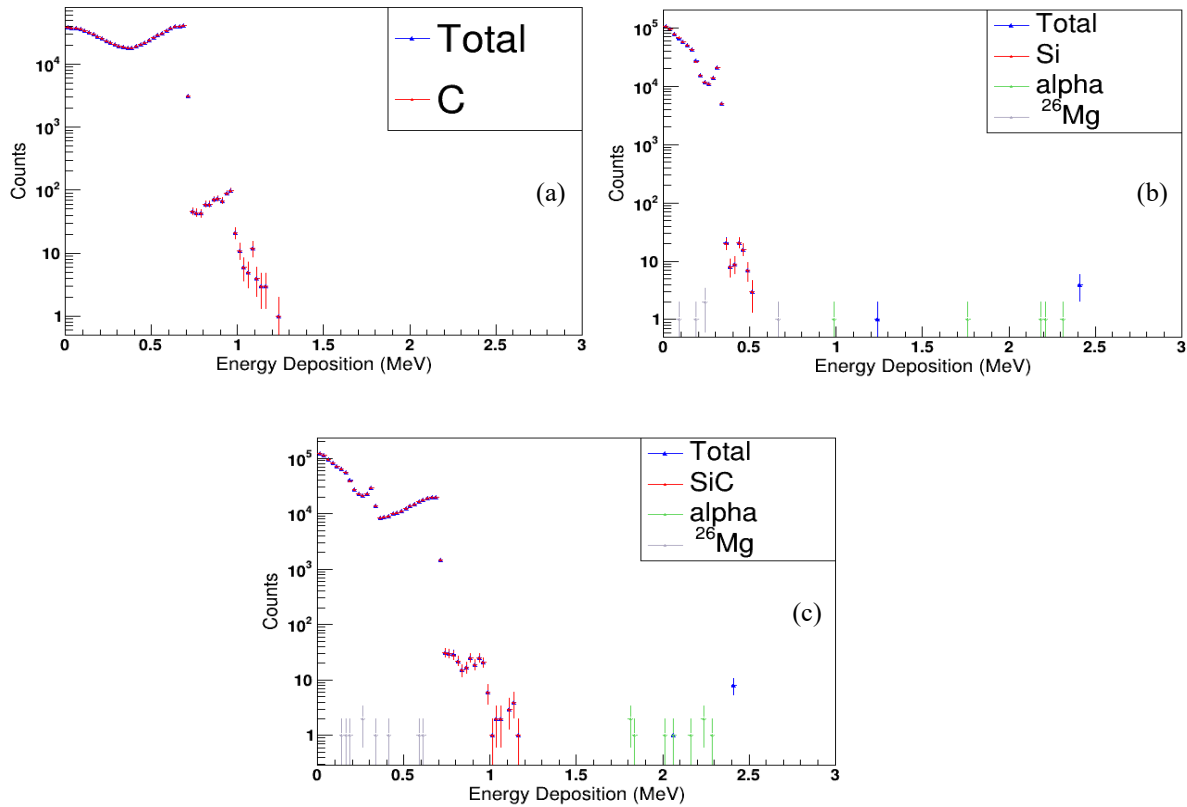


Figure 2. Energy deposition spectrum for a 50 μm C (a), Si (b) and SiC (c) detector to 2.45 MeV neutrons. The blue points represent the total energy deposition, the red the corresponding material, the green the alpha particles and the gray the ^{26}Mg nuclei.

It is essential for any detector working in neutron environments to determine how well it can distinguish γ -rays from neutron signals. Especially in a fusion reactor, γ -rays are a source of contamination and therefore an examination for a possible threshold must be performed. To this end, three typical γ -ray energies were studied: 500 keV, 1 MeV and 2 MeV and their energy deposition spectrum was collected for a 50 μm C, Si and SiC detector. The interaction probability and charge deposition with γ -rays drop significantly with increasing energy or decreasing detector thickness. For photon energy above 1 MeV, the interaction probability for a 500 μm sensor is below 1% [5], so at 50 μm sensors we don't expect contributions as the photon energy further increases. Figure 3 shows the results of the γ -rays along with the 2.45 MeV neutron spectrum for each material.

For the diamond detector in Fig. 3(a), we observe a possible threshold around 0.4 MeV. Due to the low Z of the material, it has a low interaction probability with γ -rays so the neutron signals are easily distinguished from the γ -rays. A similar behavior is observed for SiC in Fig. 3(c), because of the presence of carbon, a threshold is once again shown around 0.4 MeV. However, for Si, in Fig. 3(b), no clear threshold can be obtained. The higher Z of the material causes overlapping between the γ -rays and neutron signals for 2.45 MeV neutrons in both low and high energies.

Quasi-monoenergetic Neutron Beam

The experiment will be performed at the neutron production facility of the Tandem accelerator at the I.N.P.P. of the NCSR "Demokritos". The neutron production facility produces quasi-monoenergetic neutron beams by the interaction of light ions with gaseous or solid targets, depending on the neutron energy of interest. For the production of 2.45 MeV neutrons a solid TiT target is used and the neutron beam is produced through the $^3\text{H}(p,n)$ reaction.

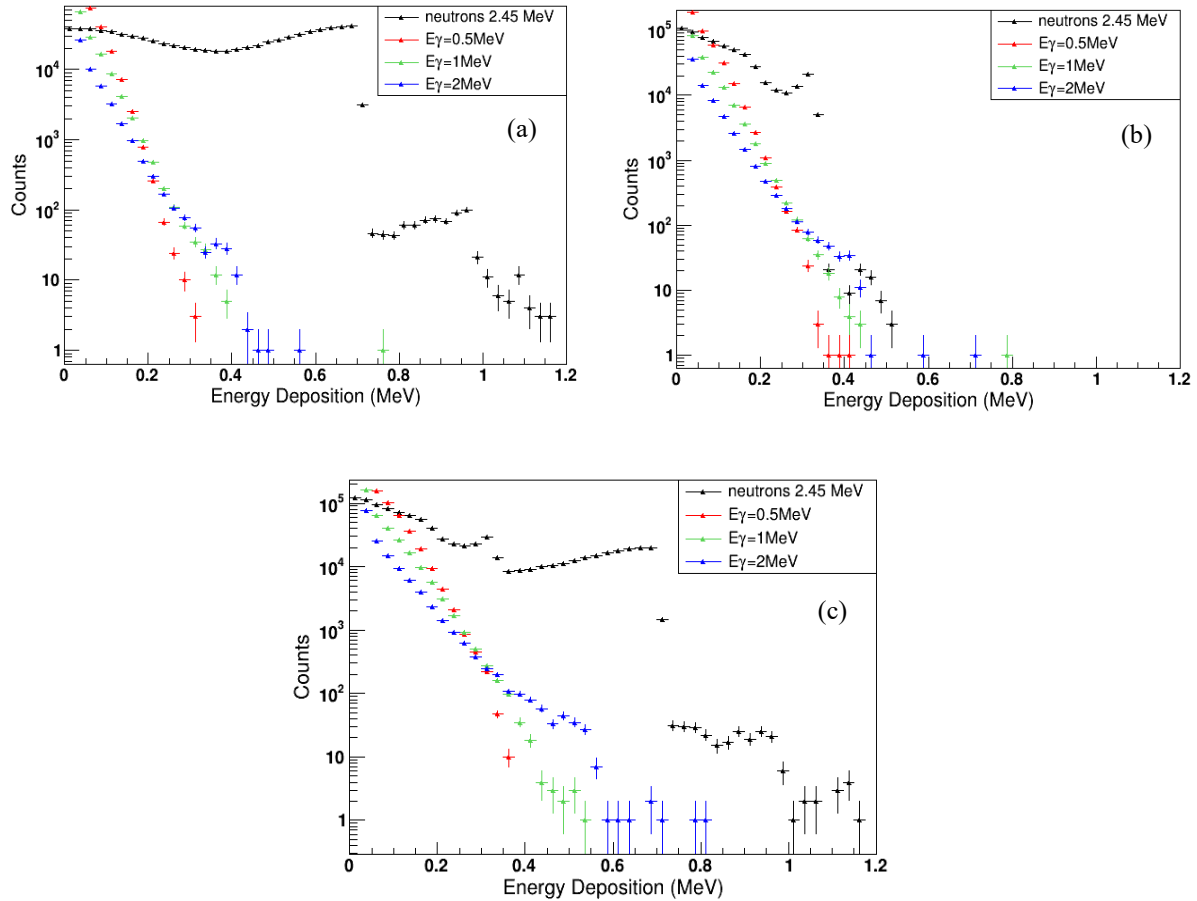


Figure 3. Energy deposition spectrum for 500 keV, 1 MeV and 2 MeV γ -rays in a 50 μm C (a), Si (b) and SiC (c) detector. The black points represent the 2.45 MeV neutron energy deposition spectrum.

In order to proceed with the GEANT4 simulations, the experimental line was built, where the passage of protons through the collimator and anti-scatterer is simulated until they reach the solid TiT target in an aluminum flange. Inside the flange the protons first encounter a thin molybdenum foil with total thickness of 0.0005 cm and radius of 1.425 cm, which acts as the entrance window. Its role is to moderate the incident proton energy so that higher proton energies can be accelerated leading to higher proton flux intensity and consequently to higher neutron flux. Immediately after the molybdenum, the TiT solid target is placed, where the main (p,n) reactions occur and the majority of neutrons is produced. This target consists of 42.8% tritium and 57.1% titanium and has a density of 3.75 g/cm³, a thickness of 0.00057 cm and a radius of 1.27 cm. The titanium confines the ³H gas in the solid target. Right after the TiT target, a foil of copper is placed, with thickness of 0.05 cm and radius of 1.425 cm, which acts as the beam stop for protons. Parasitic neutrons can be produced by (p,n) interactions in both the Mo and Cu foil or in Ti, however for the production of 2.45 MeV neutrons, these parasitic reactions are negligible. The detector with dimensions 4 mm \times 4 mm \times 50 μm was placed at 1 cm distance from the end of the aluminum flange. The material was carbon, silicon or silicon carbide respectively, for comparing the response of the different materials.

In the simulation, the proton beam with $E_p=3.805$ MeV containing 10^9 primaries is generated at the beginning of the line, while scoring the neutron energy deposition in the sensor. Due to the low cross section, a very small number of neutrons is generated and only 4 to 5 manage to deposit energy

in the detector. In order to obtain high statistics in the simulated spectra, the implementation of biasing techniques was necessary.

There is a few possible biasing techniques available in the GEANT4 code. The one chosen reduces the mean free interaction length (λ) between two consecutive interactions in a certain volume. This reduction is done by multiplying the quantity $1/\lambda$, i.e the macroscopic cross section (Σ_t), with a factor which is called biasing factor. In this way, we manage to increase the macroscopic cross section, while simultaneously reducing the mean interaction length, enabling rare events such as $^3\text{H}(p,n)$ reactions to happen with higher probability. Nevertheless, this type of biasing interferes with the distance in which the interaction takes place, altering some of the physical processes.

An increase in the biasing factor, which means a decrease in the mean interaction length, results to all the possible interactions taking place on the surface of the target. In this way the kinematics and the energy distribution can be significantly altered and deviate from the unbiased simulation. These deviations strongly depend on the shape of the cross section. If the cross section is relatively smooth, the variation in energy will cause small deviations, however when it exhibits intense resonance, the differences with the unbiased case will dramatically increase as will be shown later in the text. Consequently, the use of biasing should always be done with caution and extra tests must be performed in order to minimize the deviation from the unbiased simulation.

The implementation of biasing was first attempted in the TiT target in order to produce a realistic neutron beam through $^3\text{H}(p,n)$ reactions. In the case of a thin volume, where the particles lose a small portion of their initial energy, a high biasing factor can be used, however the cross section must always be checked. The TiT target has a thickness of 5.7 μm , so the energy loss expected from biasing will be very low. The protons after the Mo foil enter the TiT target with $E_p=3.314$ MeV, where the cross section for $^3\text{H}(p,n)$ has its highest value [6]. The value of the cross section will be altered to a very small extent given its shape and the small energy loss due to the target's low thickness. Consequently, a high biasing factor of 900 was used for biasing the primary protons inside the TiT target. The neutron energy distribution of the high statistics quasi-monoenergetic neutron beam can be found in Fig. 4, where we also observe the different contributions from the TiT target, and the Mo and Cu foils.

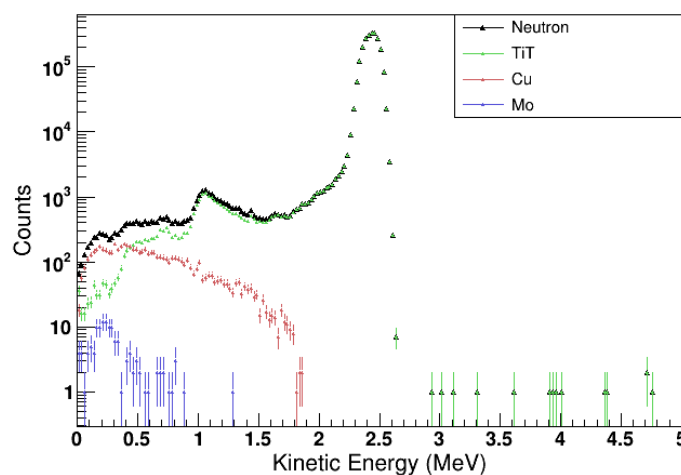


Figure 4. Final neutron beam deriving from biasing the TiT target by proton biasing factor=900, with contributions from the Mo and Cu foils

We observe that the main neutron production derives from $^3\text{H}(p,n)$ reactions, resulting in the 2.45 MeV peak. The contribution of the neutrons generated in the Cu and Mo foils is approximately 0.3% and 0.005% respectively, while for the TiT neutrons it is up to 99.6%. For Cu, due to its higher thickness, neutrons which are generated in the TiT target find it possible to scatter inside the Cu foil and thus appear as Cu neutrons in the final spectrum. The black points represent the final quasi-

monoenergetic neutron beam, which will interact with the detector. However, in order to collect the energy deposition spectra with sufficient statistics for the C, Si and SiC detectors, additional biasing in the neutron detection is necessary.

A series of tests were performed for the three materials in order to determine the neutron biasing factor which deviates the least from the unbiased simulation. The unbiased simulation is shown in Fig. 3 for C, Si and SiC including 10^9 primary neutrons and the goal is to reproduce these spectra by biasing the neutron detection inside each detector. The tests include a certain chosen number of primary neutrons and biasing factor so their product will be 10^9 and thus the deviation from the unbiased case can be found. Table 1 summarizes the results for the three materials.

Table 1. Different combinations of neutron biasing factors and primary neutrons and the deviation from the unbiased simulation of 10^9 unbiased neutrons for a 50 μm C, Si and SiC detector.

Primary Particles	Neutron Biasing Factor	Si Deviation from unbiased case	SiC Deviation from unbiased case	C Deviation from unbiased case
10^6	1000	38.32%	41.63%	31.46%
2×10^6	500	31.21%	29.53%	17.75%
2.5×10^6	400	29.69%	26.83%	14.67%
3.33×10^6	300	26.48%	23.88%	11.39%
5×10^6	200	26.21%	20.68%	7.76%
10^7	100	24.42%	17.32%	4.12%
2×10^7	50	23.34%	12.93%	-
10^8	10	20.87%	12.24%	-
5×10^8	2	11.56%	7.03%	-

We observe that as the number of primary neutrons increases and the biasing factor decreases, the deviation from the analogue case decreases as well. For the purpose of this work, emphasis was given on a small deviation from the unbiased case, in order to produce an accurate energy deposition spectrum. For Si and SiC, high deviations are observed and only the smallest possible biasing factor of 2 can be used causing a 11.56% and 7.03% deviation, respectively. For C, the chosen biasing factor was 100, causing a deviation of only 4.12%, so no further tests with lower biasing factors were necessary. The reason behind the high deviations observed in Si in contrast to C lies in the shape of the cross section. The cross section for Si elastic scattering exhibits intense resonances in the neutron energy range of interest, whereas C has a smooth cross section.

RESULTS AND DISCUSSION

Once the correct biasing factor for biasing the neutron production and the neutron detection was determined, the energy deposition spectra for the C, Si and SiC detector were produced as shown in Fig. 5, which also contains the unbiased case. The unbiased spectrum represents the simulations with a 2.45 MeV monoenergetic neutron pencil beam, described in the previous sections, while the biased spectrum results from the quasi-monoenergetic neutron beam as shown in Fig. 4, including neutron energies from 0 to approximately 2.5 MeV with a mean value of 2.405 MeV.

For C in Fig. 5(a), where a high biasing factor of 100 was used, some differences are observed between the unbiased and the two-stage biased simulation. First, the biased spectrum extends to higher energies in contrast to the unbiased. Implementing a high biasing factor will cause the majority of interactions to occur close to the target's surface. Because of the favorable cross section and the non-negligible dimensions of the sensor, the probability for two or three consecutive elastic scatterings inside the C target is increased. Consequently, multiple scatterings are observed inside the target, thus leaving a higher energy deposition compared to the unbiased case. This phenomenon causes a gap at the energy range of 0.3 MeV-0.5 MeV where the biased spectrum is below the unbiased. A neutron

scattered in 90° , which produces a recoil nucleus with energy between 0.3 MeV to 0.5 MeV, is more likely to undergo further elastic scatterings as it crosses the target due its large width (4 mm) thus leaving a gap in these energy ranges. This valley is due to the neutrons lost to double and triple scattering which are found in the tail of the C spectrum. If we reduce the thickness of the detector or the biasing factor, the probability of these elastic scatterings decreases, and the valley is shifted towards the unbiased spectrum.

For Si (Fig. 5(b)) and SiC (Fig. 5(c)), the smallest possible biasing factor of 2 was chosen according to Table 1. Some biased counts are above and some below the unbiased spectrum, due to the use of a realistic quasi-monoenergetic neutron beam and thus the contribution of a variety of neutron energies. Similar deviations are observed as in the C case, however for Si and SiC the biased spectrum seems to stop at the same energy as the unbiased one, instead of extending to higher values. Due to the low biasing factor used, the multiple scattering effect cannot occur.

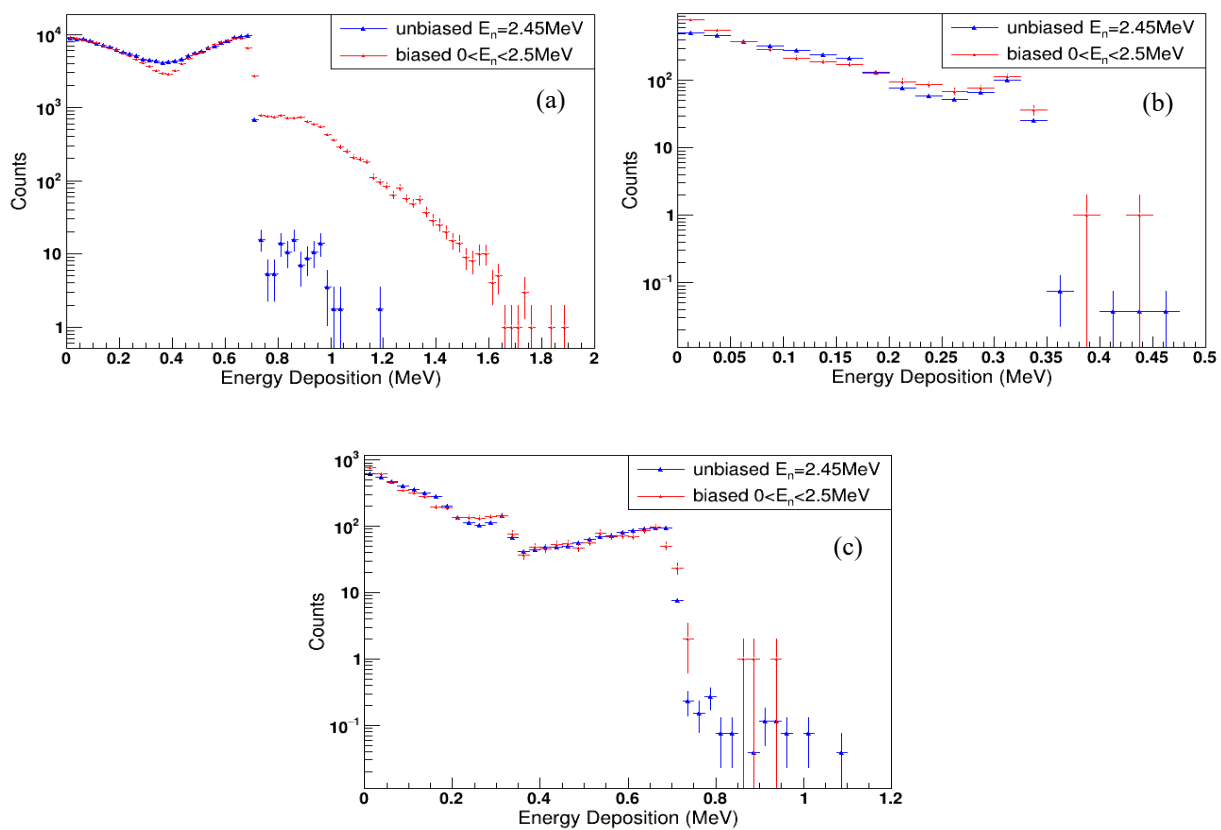


Figure 5. Energy deposition spectrum for 2.45 MeV neutrons for a $50\ \mu\text{m}$ C (a), Si (b) and SiC (c) detector. The blue points derive from a 2.45 MeV monoenergetic neutron beam with 10^9 primary neutrons. The red points correspond to 10^9 primary protons interacting with the TiT target and producing a variety of neutrons with mean energy of 2.4 MeV.

CONCLUSIONS AND FUTURE PERSPECTIVES

In this work the study of a C, Si and SiC detector to 2.45 MeV fusion neutrons was performed using GEANT4 simulations and the first results are shown. The neutron production setup of the I.N.P.P. of the NCSR “Demokritos” was built, where the experiment will be conducted with detectors provided by the CIVIDEC Instrumentation GmbH. The realistic neutron source deriving from (p,n) reactions with a TiT target was simulated and the energy deposition spectra were obtained for $50\ \mu\text{m}$ Si, C, SiC detector using biasing techniques. Throughout this investigation, it was understood that the biasing

factor strongly depends on the shape of cross section. A γ -ray study was also performed, and it was observed that Si is not an appropriate detector material for 2.45 MeV neutrons due to the strong γ -ray overlapping.

The future perspectives for the continuation of this work include the development of the GEANT4 code so the input file will be the neutron beam deriving from (p,n) reactions in the TiT target, thus reducing both the systematic error of the simulation, as well as the computing time. Development of the realistic geometry of the detector including the metallisation layers must also be made, instead of considering only the sensor volume of the detector. Lastly, the validation of the results of the simulation by conducting the experiment at NCSR “Demokritos”, and further study of the production of 14 MeV neutrons deriving from the main D-T fusion reaction is foreseen.

Acknowledgments

This work was supported and encouraged by all the members of the NTUA nuclear physics group and our colleagues from NCSR “Demokritos” in many different ways. We would especially like to mention Dr. Cristina Weiss who stimulated and encouraged the beginning of this research activity.

References

- [1] S. Agostinelli et al., Nucl. Instrum. Methods Phys. Res. A 506, 250 (2003)
- [2] K.S. Krane, Introductory Nuclear Physics, John Wiley & Sons (1991)
- [3] V. Krasilnikov, L. Bertalot, R. Barnsley, M. Walsh, Fusion Sci. Technol. 71, 196 (2017)
- [4] L. Bertalot, R. Barnsley, M.F. Direz et al., J. Instrum. 7, C04012 (2012)
- [5] P. Kavrigin, Neutron spectroscopy with sCVD diamond detectors, PhD thesis, TU Vienna (2018)
- [6] H. Liskien, A. Paulsen, At. Data Nucl. Data Tables 11, 569 (1973)